Cenozoic sediment budget of West Africa and the Niger delta

Jean-Louis Grimaud, Delphine Rouby, Dominique Chardon, Anicet Beauvais

Cenozoic sediment budget of West Africa and the Niger delta

Jean-Louis Grimaud[1,2 *], Delphine Rouby[1], Dominique Chardon[1,3], Anicet Beauvais[4]

(1) Géosciences Environnement Toulouse, Université de Toulouse, CNRS, IRD, UPS, CNES, F-31400 Toulouse, France

(2) now at MINES ParisTech, PSL Research University, Centre de Géosciences, 35 rue St Honoré, 77305 Fontainebleau Cedex, France

(3) IRD and Département des Sciences de la Terre, Université Ouaga I Professeur Joseph Ki-Zerbo, 01 PB 182 Ougadougou 01, Burkina Faso

(4) Aix-Marseille Univ, CNRS, IRD, Coll France, CEREGE, BP 80, 13545 Aix-en-Provence, Cedex 4, France

* corresponding author: jean-louis.grimaud@mines-paristech.fr

Manuscript submitted to ***Basin Research,*** 25-Nov-2016

Revised manuscript, submitted 24 April 2017

Accepted, 11 June 2017

DOI: 10.1111/bre.12248

Keywords: Source-to-sink, Cenozoic, sediment flux, Africa, craton, continental margin

ABSTRACT

Long-term (10^{6-7} yr) clastic sedimentary fluxes to the ocean provide first-order constraints on the response of continental surfaces to both tectonic and climatic forcing as well as the supply that builds the stratigraphic record. Here we use the dated and regionally correlated relict lateritic landforms preserved over Sub-Saharan West Africa to map and quantify regional denudation as well as the export of main catchments for 3 time intervals (45-24, 24-11 and 11-0 Ma). At the scale of West Africa, denudation rates are low (~7 m Myr^{-1}) and total clastic export rate represents 18.5 x 10^3 km^3 Myr^{-1}. Export rate variations among the different drainage groups depend on the drainage area and, more importantly, rock uplift. Denuded volumes and offshore accumulations are of the same magnitude, with a noticeably balanced budget between the Niger River delta and its catchment. This supports the establishment of the modern Niger catchment before 29 Ma, which then provided sufficient clastic material to the Niger delta by mainly collecting the erosion products of the Hoggar hotspot swell. Accumulations on the remaining Equatorial Atlantic margin of Africa suggest an apparent export deficit but the sediment budget is complicated by the low resolution of the offshore data and potential lateral sediment supply from the Niger delta. Further distortion of the depositional record by intracontinental transient storage and lateral input or destabilization of sediments along the margin have been identified in several locations, prompting caution when deducing continental denudation rates from accumulation only.

INTRODUCTION

Clastic sediments fluxes represent the bulk terrigenous supply to oceanic basins derived from the dissection and erosion of continental surfaces (Fig. 1). They build the sedimentary record along continental margins over geological timescale (10^{5-7} yr) and, together with chemical fluxes, contribute to the global bio-geochemical cycles. The stratigraphic record may allow retrieving paleo-environmental information such as the climatic variations, landform evolution and vertical movements on the adjacent continental domains (Burbank, 1992; Molnar, 2004; Clift, 2010), documenting the long-term response of landscapes to external forcing. Comprehensible clastic fluxes are therefore first-order data to geomorphologists, sedimentologists and geodynamicists to decipher sediment production, transfer and deposition in its ultimate basin sinks (Allen, 2008; Fig. 1).

Clastic fluxes are usually obtained from sedimentary basin accumulations (e.g. Rust & Summerfield, 1990; Métivier et al., 1999; Guillocheau et al., 2012). Stratigraphy alone however lacks information about catchment evolution (Bishop, 1995) and distribution of erosion within the source region. Furthermore, temporary storage and later erosion of sediments may delay or erase stratigraphic information (Sadler, 1981; Métivier & Gaudemer, 1999; Jerolmack & Paola, 2010). Sediment fluxes predicted from landscape evolution models are calibrated at micro- to mesoscale (m^2 to km^2) and short-term (10^{1-4} yr), and may not be representative of large continental surfaces ($> 10^4$ km^2) evolving at geological timescale (Simoes et al., 2010). Sediment budgets comparing source and sink are therefore the most meaningful to understand relief dynamics at geological timescales but are limited by the lack of constraints on the source catchments and require making assumptions on their topographic and drainage evolution (e.g. Leturmy et al., 2003; Campanile et al., 2008; Rouby et al., 2009; MacGregor, 2013). Better

67 constraints on continent-scale surface evolution are required to calibrate long-term clastic fluxes
68 and the associated sedimentary basin evolution.

69 Cratons represent low-lying, slowly eroding domains (Bishop, 2007; Beauvais &
70 Chardon, 2013) but integrate large continental catchments (i.e. 10^6 km^2; Fig. 2). Cratons are the
71 source of major clastic accumulations over long-lasting segments of passive margins in Africa
72 and worldwide, hosting extensive sediment archives as well as hydrocarbon resources (Bradley,
73 2008). The slow erosion rates of cratons result in the preservation of geomorphic markers as
74 illustrated by the relicts of lateritic landscapes of tropical shields derived from Meso-Cenozoic
75 intense weathering periods associated to warm climate (Tardy & Roquin, 1998; Zachos et al.,
76 2001; Beauvais & Chardon, 2013; Fig. 3). Quantifying erosion using these relict landforms has
77 proven useful to apprehend the denudation rates and landform evolution of cratonic sediment
78 routing systems (Beauvais & Chardon, 2013; Grimaud et al., 2015).

79 This study presents a comparison between the volumes eroded and exported from the
80 main catchments of Sub-Saharan West Africa and the sediments preserved in the adjoining
81 continental margin basins of the Equatorial Atlantic Ocean during the Cenozoic. We use relict
82 lateritic landforms and recently published paleo-drainage maps (Chardon et al., 2016) to
83 constrain continental clastic exports, and a measure of offshore accumulations. We compare
84 accumulation with erosion between the Niger delta and its catchment and between the remaining
85 portion of the Equatorial Atlantic margin of Africa (i.e. without the Niger delta) and its sources.
86 Accumulated and eroded volumes fall within the same range allowing discussion of the influence
87 of rock uplift, catchment evolution and sediment transfers on sediment budgets.

88

89 **GEOLOGICAL SETTING AND EARLIER WORK**

90 The studied area comprises a 4 x 10^6 km^2 cratonic surface extending from the Senegal-
91 Mauritania basin to the west and to the Hoggar and Adamaoua massifs to the northeast and
92 southeast, respectively (Fig. 2). Major river systems (the Niger, Senegal and Volta rivers)
93 currently collect sediment supplied to the continental margin basins of this domain. The Niger
94 catchment (2.3 x 10^6 km^2) drains the main topographic massifs: the Guinean rise, the southern
95 Hoggar massif and the Jos plateau and the Adamaoua massif bounding the Benue trough (Fig. 2).
96 At the outlet, the Niger delta surface is 26 x 10^3 km^2 and its Cenozoic sediment thickness exceeds
97 9 km (Fig. 2). In contrast, the remaining portion of the Equatorial Atlantic of Africa (i.e.
98 excluding the Niger delta; Fig. 2), fed by rivers such as the Volta, has a larger basin surface (750
99 x 10^3 km^2) and a thinner Cenozoic sediment cover (< 3 km; Helm, 2009).

100 The West African bedrock is composed of Archean and Paleoproterozoic basement
101 bounded by mobile belts of Panafrican (~800 – 450 Ma) and Variscan (~360 – 250 Ma) ages
102 (Villeneuve, 2005; Feybesse et al., 2006). It is overlain by Neoproterozoic to Phanerozoic
103 sedimentary series, the main depocenter of which is located in the Taoudeni basin (Villeneuve,
104 2005; Fig. 2). Cenozoic sedimentary series preserved onshore include Eocene carbonates found
105 in the Senegal-Mauritania, Iullemmeden and Togo-Benin basins overlain by Lutetian to Rupelian
106 (49–29 Ma) continental deposits known as the Continental Terminal (Chardon et al., 2016). Sub-
107 Saharan West Africa is considered as tectonically stable since Late Cretaceous rifting in the
108 Iullemmeden, Chad and Benue basins, and has mostly undergone long-wavelength lithospheric
109 deformation since (Ye et al., 2017 and references therein). The Central Atlantic Ocean opened
110 since the Late Triassic and the Equatorial Atlantic during the Late Early Cretaceous (Brownfield
111 & Charpentier, 2006; Moulin et al., 2010; Labails et al., 2010; Ye et al., 2017; Fig. 2). The
112 offshore Cenozoic stratigraphic record in West Africa is characterized by a shift in sedimentation

during the Oligocene. The Paleocene-Eocene was a period of relatively high sea level, intense inland weathering and preferential deposition of chemical sediments (i.e. carbonates and phosphates) in the intracratonic and marginal basins (Fig. 3) (Millot, 1970; Valeton, 1991). The Oligo-Miocene period marked the increase of clastic sedimentation in continental basins and adjacent passive margins (Séranne, 1999; Burke et al., 2003). A paleo-Niger delta was likely established in the Benue during the Paleocene (Reijers, 2011) but the main delta progradation started at 34 Ma (Doust & Omatsola, 1990). In the literature, the Oligocene shift in sedimentation has been interpreted as resulting from either the effect of greenhouse to icehouse climatic transition (Séranne, 1999) or to the continental uplift of Africa contemporaneous with the development of its "basin-and-swell" topography driven by the growth of several hotspot swells such as the Hoggar, the Adamaoua or the Jos Plateau (Burke, 1976, 1996; Burke et al., 2003; Fig. 2). Using the reconstructed geometries of dated paleolandscapes, Chardon et al. (2016) suggested the establishment of the modern Niger River watershed in, at least, the Late Oligocene (29 Ma) and possibly the Eocene-Oligocene boundary (34 Ma) i.e., at the acceleration of the progradation of the Niger delta. The major drainage reorganization and the growth of the Hoggar hot spot swell would explain the increase in clastic fluxes toward the Niger Delta (Chardon et al., 2016). Post-Eocene clastic fluxes would also have been increased by uplift-related erosion along a marginal upwarp inherited from Mesozoic rifting that extended from the Jos Plateau to the Guinean rise (Beauvais & Chardon, 2013). The marginal upwarp is a 300 to 800 km wide strip of relief, running parallel to the coast. It is interpreted as initiating during the rifting and maintained by lithosphere flexure, erosional unloading and associated sediment loading on the adjoining margin (Gilschrist & Summerfield, 1994; Beaumont et al., 2000).

DENUDATION CHRONOLOGY

Sub-Saharan West Africa was located within the tropical belt throughout the Cenozoic, allowing several generations of lateritic regoliths to be produced regionally. Rivers removed parts of these regoliths to form a unique geomorphic sequence of stepped paleolandscapes capped by duricrusts (Michel, 1973; Fig.3a). These landscapes were not sub-continental flat planation surfaces as advocated by King (1962) but composite landscapes, the relief of which increased throughout the Cenozoic (Figs. 4 and 5; Beauvais & Chardon, 2013; Grimaud, 2014; Grimaud et al., 2015). Each member of the sequence has a specific morphology and type-regolith that reflect variation of weathering intensity and slope erosion processes (Boulangé et al., 1973; Grandin, 1976; Tardy & Roquin, 1998). This allows for correlations of each type of paleo-landscape remnant on a regional scale (e.g. Fig. 4; Beauvais & Chardon, 2013; Grimaud et al., 2014). The regolith formed by lateritic weathering of the bedrock during long ($>10^6$ yr), warm and humid climatic periods (Fig. 3b). Weathering resulted in leaching of mobile elements and the accumulation of less mobile iron and/or aluminum in the shallow depths of the regolith profiles. Ultimately, the duricrusting of the upper horizons occurred when the weathering profiles became disconnected from the local base levels (i.e., following river incision and/or the return to drier climatic conditions). Hence, the terminal weathering age of a regolith profile capped by a duricrust is considered as marking the abandonment of the associated paleo-surface (i.e. Fig. 3).

The first member of the West Africa geomorphic sequence (S1; Fig. 3) is a surface of continental scale, known as the “African Surface”, formed under a humid equatorial climate from the Late Cretaceous to the Eocene (Beauvais & Chardon, 2013). Weathering shaped a low-relief landscape and formed bauxites (i.e. Al-Fe crust; Figs. 3 and 4). The S1 bauxite was abandoned to form an incised landscape during the development of the next member of the sequence, the so-

called “Intermediate” surface (S2; Fig.3), ultimately capped by a ferricrete. The S2 surface was dissected and abandoned during the development of the S3 erosion surface (“High glacis” in the French literature). S3 is a pediment, i.e., a gently sloping concave-upward surface, formed under semi-arid to arid climate during which stable base level and high seasonality favor surface sheetwash during the monsoon (Hadley, 1967; Grandin, 1976). Ferricretes capping S3 formed under more contrasted humid conditions (Fig. 3b). S3 ferricrete often cements a detrital layer that contains clasts of S1 and S2 crusts (Boulangé et al., 1973; Grandin, 1976; Grimaud et al., 2015). Hence S1, S2 and S3 remnants have first order distinctive landform-regolith associations that allow for regional correlation (Beauvais & Chardon, 2013; Grimaud et al., 2014).

Ages of laterite formation were bracketed by ^{40}Ar-^{39}Ar dating of supergene K-rich Mn oxides such as cryptomelane $[K_x (Mn^{3+})_x (Mn^{4+})_{8-x} O_{16}]$ in Tambao, Burkina Faso (Beauvais et al., 2008), and sulphates as alunite / jarosite in Syama, Mali (Vasconselos et al., 1994a; Fig. 3b). These minerals formed under weathering and oxidation conditions converting the bedrock into lateritic regolith and are therefore useful tracers of major weathering periods and associated formation of duricrusted surfaces. The S1 surface was abandoned after 45 Ma, S2 after 24 Ma and S3 after 11 Ma (Beauvais & Chardon, 2013; see also Grimaud et al., 2015; Figs 3 and 4). The radiometric ages of the West African geomorphic sequence (Fig. 3b) are consistent with other time-constraints. The weathering of the bauxitic paleolandsurface is correlated to chemical marine sedimentation in Sub-Saharan West Africa during the Early-Mid Eocene interval (Millot, 1970), while the S2 ferricrete caps the weathering profiles developed upon Late Eocene-Oligocene “Continental Terminal” alluvial deposits (Chardon et al., 2016).

MEASURE OF CONTINENTAL DENUDATION AND SEDIMENT EXPORT

Regional distribution and mapping of lateritic relict landforms

We referenced S1, S2 and S3 relicts over West Africa (Fig. 5) using a combination of fieldwork (in Benin, Burkina Faso, Mali, Niger, Guinea and Senegal), descriptions from existing literature (e.g. Newill & Dowling, 1968; Fölster, 1969; Eschenbrenner & Grandin, 1970; Boulangé & Eschenbrenner, 1971; Michel 1973, 1977a, 1977b; Boulangé et al., 1973; Grandin & Hayward, 1975; Grandin, 1976; Burke, 1976; Fritsch, 1978; Thomas, 1980; Rognon et al., 1983; Adegoke et al., 1986; Bowden, 1987; Boulangé & Millot, 1988; Durotoye, 1989; Teeuw, 2002; Thomas, 1994) (recent compilations in Beauvais & Chardon, 2013; Grimaud, 2014) and combined analyses of topography and satellite images. Field stations and the full compilation of the references can be found in the Supporting Information. We identified and reported the elevation of S1, S2 and S3 remnants based on their geomorphology and regolith type (see below). In order to further constrain the regional geometries of the surfaces, we also surveyed additional data such as topographic massifs summits (B points), Early-Mid Eocene carbonates (C points) and lower parts of S1 weathering profile remnants (D points) (Chardon et al., 2016). Figure 5 illustrates how these data points were used to reconstruct surface geometries.

S1 relicts dominate West African landscapes in the form of bauxitic mesas capped by a flat duricrust of beige to pink color reflecting the presence of aluminum (Figs. 4a and 5b). In the Guinean rise and eastward (i.e. upwarp domain; Fig. 2), the S1 relicts are preserved 400 to 600 m above modern rivers (see Beauvais & Chardon, 2013). This local relief decreases towards the coast and the continental interiors, where S1 relicts are less than 60 m above the Niger River in the Inland Niger delta (Grimaud et al., 2014; Figs. 2 and 4c).

S2 ferricretes have red-purple colors on satellite images due to their high iron content and a morphological aspect different from S1 and S3 (Figs. 4 and 5b). S2 relicts are usually

distributed 50-200 m, and locally up to 400 m, vertically in the landscape below S1 remnants (Grandin, 1976; Beauvais & Chardon, 2013). They are either connected to bauxite relicts, forming convex-upwarp surface on the slopes of S1 mesas (Figs. 3a, 4a, 4b and), or occur stepped under S1 relicts. It has been shown that the elevation of S2 relicts decreases from the divides to the outlet of West African catchments, following the geometry of the main watersheds and implying that the S2 drainage was similar to the modern one (Beauvais & Chardon, 2013; Grimaud et al., 2014; Chardon et al., 2016; Figs. 4a, 4b and 4d).

S3 ferricretes can usually be identified in the field by their embedded conglomerate deposits and their brown to grey color on satellite images. S3 relicts usually form gently dipping plateaus of several square kilometers in area with concave-up profiles (Figs. 3a and 4). S3 plateaus are easily identified when radiating from the piedmont of S1 or S2 mesas (Figs. 4a and 4b). The downstream parts of S3 relicts are usually 10-100 m above modern rivers and well preserved throughout West Africa, suggesting modest post-11 Ma landscape dissection and denudation (Beauvais & Chardon, 2013; Grimaud et al., 2015; Fig. 4).

Quantification of exported volumes and conversion to sediment fluxes

We estimated denudation volumes and the associated export to offshore basins using regional reconstructions of S1, S2 and S3 surface geometries, and the modern topography. S1, S2 and S3 geometries were reconstructed using the DSI method (Mallet, 1992) that allows building complex geologic surfaces (see Chardon et al., 2016). By subtracting these surfaces, we obtained the S1-S2, S2-S3 and S3-modern elevation differences maps corresponding to incremental denudation maps for the 45-24, 24-11 and 11-0 Ma intervals (Fig. 6) as well as the total

227 denudation map since 45 Ma (i.e. S1-modern map; Fig. 7). S1 and S2 surfaces geometries are
228 those published by Chardon et al. (2016) and S3 surface is from this study.

229 The sediment volumes stored in continental sedimentary basins during the S1-S2 interval
230 (blue colors on Figure 6b) were subtracted to the eroded volumes to obtain the volumes exported
231 to the continental margin (V_{ex}) (Table 1). These storage volumes were calculated between the S1
232 and S2 surface geometries. They are actually larger than the volumes currently preserved in the
233 intracratonic sedimentary basins because of erosion after 24 Ma (see Fig. 8 for an illustration in
234 the Iullemmeden basin).

235 We developed an analysis of uncertainties on the exported volumes estimates. Overall, we
236 found errors values around 10-30% (see Table 1 and Supporting Information). The first
237 uncertainty was estimated for the construction of surface geometries. For that, we built replicates
238 of the S2 and S3 surfaces, respectively S'2 and S'3, to measure the variability of their geometries.
239 S'2 and S'3 are less realistic and less elevated than S2 and S3 surfaces (Figs. SI2 and SI3)
240 because they were built using only S2 or S3 points respectively, i.e. they were not enforced at the
241 location of the anterior surfaces or forced by the topography. The uncertainties on surface
242 geometries were then measured by the elevation difference between S2 and S'2 and S3 and S'3
243 (Fig. SI3).

244 The second uncertainty related to the partitioning of erosion volumes of denudation maps,
245 built at the scale of West Africa, between four drainage groups (Senegambia, Short Atlantic
246 drainages, Long Atlantic drainages and the Niger catchment; Fig. 6a). In this study, we used the
247 paleo-drainage maps of Chardon et al. (2016), where the drainage divide positions themselves are
248 located within an area of uncertainty (i.e. Figs. 6b and 6c). We calculated the volume eroded
249 within this uncertainty area to estimate the volume uncertainty associated to the divide location.

The last uncertainty was associated to the type of exported material. Lateritic regolith represents the type-material eroded from the West African continental domain during the Cenozoic (Beauvais and Chardon, 2013). The density and porosity of the eroded lateritic regolith is different from bedrock (e.g. Grimaud et al., 2015). Exported volume (V_{ex}) was corrected for the lateritic regolith porosity, φ, which varies from 10 to 40 % (Valeton, 1991; Boulangé, 1984; Beauvais & Colin, 1993; Thomas, 1994). We thus estimated the clastic exported solid volume assuming a 25% mean porosity in the regolith (Table 1). Regolith bulk density is 2,000 kg m^{-3} (Valeton, 1991), which corresponds to a grain density ρ of 2,650 kg m^{-3}. We estimate the clastic yields γ of each drainage group using:

$$\gamma = \frac{V_{ex}.(1-\varphi).\rho}{1000.A.\Delta_t} \quad (1)$$

where A and Δ_t are the catchment area and the time-interval, respectively, and γ has unit of mass per unit area per time (t km^{-2} yr^{-1}). Calculations of clastic exported solid volumes and clastic yields therefore assumed that most eroded material was regolith. Because in West Africa bedrock outcrops are rare, erosion rates are slow and regolith mantles are thick, the assumption seems reasonable (Grimaud et al., 2015). This also implies that a sizeable portion of the denuded volume, which we did not quantify, was exported as solute load. However, in area with fast denudation rates, the eroded material may locally be only moderately weathered. In that case, the actual clastic export was higher than our estimate, which should therefore be considered as minimum.

OFFSHORE CLASTIC ACCUMULATION ON THE MARGIN(S)

271 Offshore accumulations were calculated in term of solid volumes (i.e., corrected for
272 porosity and non-clastic material such as volcanics and carbonates) following the method of
273 Guillocheau et al. (2012), based on regional geological cross-sections (Fig. 9). The calculation
274 technique, non-clastic material and remaining porosity corrections, and uncertainties estimations
275 are presented in the Supporting Information.

276 In the Niger delta domain, we used the four sections published by Haack et al. (2000) that
277 encompass most of the Cenozoic depocenters (Figs. 9a and 9b). Given the biostratigraphic age
278 constraints available for the sediments, these sections allowed measuring accumulation at higher
279 time resolution ($10^{5\text{-}6}$ yr; Fig. 9d; Table 2) than the denudation maps. Hence, we recalculated
280 accumulations for the 45-23, 23-11.6 and 11.6-0 Ma intervals to allow for comparison with the
281 erosion chronology (Fig. 9e; Table 2). In the Equatorial Atlantic, we used 6 sections (after de
282 Caprona, 1996; MacGregor et al., 2003) that only encompass the proximal parts of the margins.
283 We then used the extrapolation of these cross-sections to the abyssal plain proposed by Helm
284 (2009) (Fig. 9c; Supporting Information) to include volume accumulated across the entire
285 sedimentary wedge and to take into account erosion from, or by-pass of, the continental shelf
286 (Fig. 9f). Volume for the 45-33.9 Ma interval was recalculated using the accumulation rate of the
287 55.8-33.9 Ma interval (Table 1).

288

289 **RESULTS**

290 **Spatial and temporal denudation patterns**

291 Incremental (45-24, 24-11 and 11-0 Ma) and total (45-0 Ma) denudations are
292 heterogeneous at regional scale (i.e. Figs. 6 and 7). Overall, denudation is greater in the eastern

swells (i.e., massifs located to the east of the dashed line in Figures 6b, 6c and 6d) and along a 300 to 800 km wide strip running parallel to the coast (i.e. from the Jos Plateau to the Guinean rise and the Tagant) that we interpret as a marginal upwarp following Beauvais & Chardon (2013). Total denudation exceeds 1500 m in the Hoggar massif and ranges between 400 and 1000 m along the marginal upwarp (Figs. 7 and 8a). Elsewhere, the total denudation is usually less than 400 m. Some onshore accumulation (i.e. negative erosion) is observed in the Togo-Benin, Senegal-Mauritania and Iullemmeden basins, where up to 400 m were accumulated during the 45-24 Ma interval (Figs. 6b and 8a). Post-24 Ma denudation is low in these basins (< 100 m; Figs. 6c and 6d) with the noticeable exception of the northern Iullemmeden basin where geological sections show that at least half of the "Continental Terminal" deposits were eroded (Fig. 8a).

From 45 Ma to the present, denudation was high in the Hoggar massif with a maximum during the 24-11 Ma interval (up to 1200 m; Fig. 6). During that period, denudation was more broadly distributed (i.e. it extended toward the North Iullemmeden basin; Fig. 8a) than during the 45-24 and 11-0 Ma intervals. Denudation was more homogenously distributed on the marginal upwarp between 45 and 24 Ma than after 24 Ma. On the Guinean rise (i.e. mostly the Short Atlantic drainages group), relatively high denudation depths were maintained at all times (Fig. 6). Similarly, high denudation depths were recorded from 45 to 11 Ma by the Long Atlantic drainages group in an area that is currently lying low in comparison to the neighboring Guinean rise (Fig. 2). In the Long Atlantic drainages and Niger catchment groups, denudation depths are overall lower during the 11-0 Ma interval (Fig. 6). In the Senegambia group, denudation increased after 11 Ma in both the Tagant massif and the northwestern slope of the Guinean Rise (Beauvais & Chardon, 2013; Figs. 2 and 6d). In the Benue trough, the tabular Paleocene Kerri-

316 Kerri Formation is capped by a duricrust comparable to the Intermediate ferricrete (Newill &
317 Dowling, 1968; Adegoke et al., 1986), which allows constraining the incision of these deposits
318 after the abandonment of S2 surface (i.e. 24 Ma; Fig. 3). A geologic section suggests that Benue
319 valley denudation did not exceed 200 m since 24 Ma, corresponding to a maximum denudation
320 rate of 8.4 m Myr^{-1} (Fig. 8b).

321 These data show that denudation rates are overall low in West Africa since 45 Ma (mean
322 denudation rate of 7.4 m Myr^{-1}; Table 1). They are higher in the Hoggar massif (i.e. larger than
323 30 m Myr^{-1}) and the marginal upwarp (up to 10 m Myr^{-1}), where some temporal variations are
324 also observed. Denudation rates remain lower than 5 m Myr^{-1} in the remainder of West Africa.

325

326 **Export at the scale of major catchments**

327 In total, the West African sub-continent exported 834 x 10^3 km^3 of solid clastic sediments
328 to the ocean (Table 1) since 45 Ma. These clastic volumes were distributed between the major
329 drainage groups (Figs. 6 and 7): 74 x 10^3 km^3 from the Senegambia, 83 x 10^3 km^3 from the Short
330 Atlantic drainages, 170 x 10^3 km^3 from the Long Atlantic drainages and 430 x 10^3 km^3 from the
331 Niger catchment (Table 1). At first order, exported solid volumes therefore increase with the size
332 of the contributing area. Results also show that the export is modulated by onshore storage of
333 sediments that we subtracted. Hence 16% (12 x 10^3 km^3) of the total clastic export from
334 Senegambia is stored onshore in the Senegal-Mauritania basin whereas only 5% of the total
335 clastic export from the Niger catchment is preserved in the Iullemmeden basin. In the Niger
336 source-to-sink system, we did not measure denudation in the Benue trough and surrounding
337 massifs (Figs. 6 and 7) because the rare descriptions of regolith (Fritsch, 1978; Guillocheau et al.,

338 2015) would not allow to rigorously integrating them to the denudation chronology. However, we
339 have estimated and added a Benue trough export to compare the clastic export from the Niger
340 catchment to the accumulations in the Niger delta. We estimated that the Benue contributed a
341 solid clastic volume of ca. 187 x 10^3 km^3 assuming that the average West African denudation rate
342 of 7.4 m Myr^{-1} applies to this area (~ 0.77 x 10^6 km^2; Table 1). This rate is compatible with
343 observations in the Benue valley (see previous section). Denudation was potentially higher,
344 enhanced by Neogene uplift, in the surrounding massifs (Burke, 1976). However, the
345 preservation of Neogene volcanics and lateritic regoliths in the Jos Plateau and Adamaoua
346 massifs (Boulangé & Eschenbrenner, 1971) suggests that denudation rates were probably much
347 lower there than in the Hoggar area. In parallel, the neighboring Chad basin has been constantly
348 subsiding and trapping sediment since at least 24 Ma (Burke, 1976), suggesting that no sediment
349 was diverted from the basin into the Benue trough (see Chardon et al., 2016). Using a mean West
350 Africa denudation rate seems therefore reasonable to estimate the erosion in the area of the Benue
351 Trough. In line with these hypotheses, the resulting total clastic export of the Niger-Benue
352 catchment reaches 630 ±172 x 10^3 km^3 since 45 Ma (Table 1). The Hoggar swell area has
353 contributed ca. 66 % of this volume.

354 Temporal variations in clastic export reflect the evolution of denudation rate and drainage.
355 In most drainage groups, clastic export rates were lower during the 45-24 Ma interval than during
356 the 24-11 Ma interval (Figs. 7b-7e). Within the Senegambia drainage group, clastic export rate
357 was slightly higher in the 11-0 Ma interval. In contrast, clastic export rate was steady for the
358 Short Atlantic drainages group (Figs. 7b and 7c). In the Long Atlantic drainages group and the
359 Niger catchment, export rates were lower during the 11-0 Ma interval than during the 24-11 Ma
360 interval (Figs. 7d and 7e). The highest uncertainties on clastic export rates are estimated for in the

Long Atlantic drainages group and Niger catchment because of the major drainage reorganization between 45 and 24 Ma (Chardon et al., 2016; Table 1; Supporting Information). Hence the overall export trends among drainage groups appear regionally consistent in between the 45-24 and 24-11 Ma intervals and more contrasted in between the 24-11 and 11-0 Ma intervals.

Offshore accumulation

Offshore domains differ in their structural and sediment accumulation patterns (Fig. 9a). For the Niger delta, the sections used to estimate accumulation encompass the major part of the Cenozoic sedimentary wedge located along the margin (Fig. SI4). These sections show thick marginal clinoforms that have prograded over 150 km since the Oligocene and that are affected by faulting and folding (Figs. 8b and 9b). Along the remaining part of the Equatorial Atlantic margin, 90 % of the Cenozoic wedge is spread over the abyssal plain and extends over 300-600 km offshore (Fig. 9c).

Accumulation rates for the Niger delta can be estimated at higher resolution than denudation (Fig. 9d). These rates show a steady increase from ca. 5 to 10 x 10^3 km^3 Myr^{-1} between 45 and 16 Ma. After 16 Ma, the accumulation rates increased to more than 20 x 10^3 km^3 Myr^{-1}. A peak in accumulation rate (40 x 10^3 km^3 My^{-1}) is recorded between 5.3 and 1.8 Ma, followed by a relative decrease after 1.8 Ma (Jermannaud et al., 2010). Solid accumulation rates, re-sampled for long-term intervals, are respectively ca. 5, 12 and 28 x 10^3 km^3 Myr^{-1} during the 45-23, 23-11 and 11-0 Ma intervals. These data show that a larger volume of Neogene sediments is preserved in the delta compared to Paleogene sediments. The resulting total clastic accumulation since 45 Ma is about 580 x 10^3 km^3 (Table 2). This number is remarkably

383 consistent with -although slightly lower than- the calculated clastic volume exported by the
384 Niger-Benue catchment since 45 Ma (ca. 630 x 10^3 km^3; Table 1).

385 Along the rest of the margin, available data have a lower resolution than in the Niger
386 delta, especially in the abyssal plain, and imply larger uncertainties (Fig. 9; see Helm, 2009).
387 Accumulated volumes computed for the three time intervals suggest a long-term pattern of
388 accumulation rate comparable to that of the Niger delta. The volumes are ca. 65, 85 and 300 x 10^3
389 km^3 during the 45-33, 33-21 and 21-0 Ma intervals, respectively (Fig. 9f). The total accumulated
390 clastic volume since 45 Ma is 450 ±120 x 10^3 km^3. This is 2-4 times higher than our estimate of
391 exported clastic volumes (151 x 10^3 km^3) from the source area.

392

393 **DISCUSSION**

394 **Cenozoic sediment budget**

395 Surficial mass transfers from source to sink and the associated (un) loading of the crust
396 are key aspects of the topographic evolution and stratigraphic record of passive margins (Rouby
397 et al., 2013). Our study provides independent volumetric estimations of denudation at a sub-
398 continental scale over the Cenozoic using relict paleolandforms and of accumulation using
399 offshore regional sections. The main insight from our study is the fairly well balanced sediment
400 budget between the Niger delta and its source area. Such a finding supports the paleodrainage
401 reconstruction of Chardon et al. (2016) who suggested the establishment of the modern Niger
402 River watershed since at least the Late Oligocene (29 Ma). The modern-like Niger River
403 catchment since at least 29 Ma collected sediments from a ca. 2 x 10^6 km^2 catchment and
404 transferred the large eroded volumes derived from the Hoggar hot spot swell to the ocean. The

antiquity of the Niger catchment appears as a prerequisite to the large clastic accumulations in the Niger delta given the low denudation rates (5-30 m Myr^{-1}) at the scale West Africa.

Although our estimations fall within the same order of magnitude, we estimated a deficit on the volume of sediments exported by the Long Atlantic drainages group with respect to the accumulation along the Equatorial Atlantic margin they have fed (Fig. 9f; Table 1). Geometries of the offshore geological sections are, however, not well constrained and were deduced from low-resolution geophysical data with limited age constraints (Emery et al., 1975). Thus, an uncertainty of merely ten meters thickness on the distal geometry of a stratigraphic horizon may have significant repercussions on volume estimation in a basin as large as the Equatorial Atlantic, leading to underestimation or overestimation of accumulation. Clastic sediment budgets of the abyssal plains can further be affected by additional aeolian dust input from the Sahara (Windom, 1975), and more importantly by reworking by longitudinal bottom currents (Séranne and Nzé Abeigne, 1999; Anka et al., 2009). Some sediments derived from the Niger catchment may also have by-passed the delta toe and have been deposited on these parts of the Equatorial Atlantic, further complicating the sediment budgets. This is supported by the westward extension of the Niger delta (Fig. 2) and consistent with the fact that, in our estimation, accumulation is slightly lower than denudation in the Niger source-to-sink budget. Future studies constraining westward sediment transfer in the western Niger delta would help to decipher the apparently low export of the Long Atlantic drainages group.

We measured a difference between the volumetric accumulation rate of the Niger delta (~30 x 10^3 km^3 Myr^{-1}) and the export rate of the Niger catchment (~12 x 10^3 km^3 Myr^{-1}) during the 11-0 Ma interval (i.e. Fig. 7e and 9e). Assuming that the biostratigraphy used by Haack et al. (2000) is accurate, this difference could be explained by post-11 Ma erosion of sediments that

were previously stored within the Niger sediment routing system, particularly on the shelf. As an analogy, the widespread erosion of Miocene sediments stored on the continent or the shelf has led to such reworking on the neighboring South Atlantic margin (e.g. Lavier et al., 2001; Walford & White, 2005; Linol et al., 2014). In the study area, reworking of Cenozoic sediments is supported by the incision of large canyons in the Niger delta (Doust & Omatsola, 1990) and the removal of at least 50 % of the former "Continental Terminal" after 24 Ma in the Iullemmeden basin (see geological section in Fig. 8a). Overall, the discrepancy between accumulation and erosion is a point of caution when deducing denudation rates and paleo-sediment fluxes from the accumulation record only. Indeed, if the 11-0 Ma clastic deposits are partly composed of recycled material, their volume may overestimate continental denudation after 11 Ma, and underestimate denudation before that time.

Erosion dynamics in a non-orogenic domain

Our maps show that denudation is very heterogeneously distributed across West Africa as well as within each drainage group. Regional denudation patterns suggest an influence of long-wavelength rock uplift (> 300 km) (Figs. 7 and 8; Chardon et al., 2016). Denudation focused on the Hoggar suggests a rock-uplift pattern with > 700 km radius (Fig. 7a) related to mantle dynamics (Burke et al., 2003; Chardon et al., 2016). Recently published apatite (U-Th)/He thermochronological data indicate Cenozoic denudation in the Hoggar of 1-2 km between 78 ± 22 Ma and 13 ± 3 Ma (Rougier et al., 2013), which is consistent with our estimation (~ 1.5 km; Fig. 8a). Because we did not find the equivalent of S1 there, it is likely that we have even slightly underestimated the denudation of the Hoggar for the 45-24 Ma interval. Nevertheless, the eroded material derived from the Hoggar swell was instrumental in obtaining the volume accumulated in

451 the Niger delta. As an illustration, applying the mean denudation rate of the other drainage groups
452 (i.e. 6.6 m Myr^{-1}) over the Niger catchment for 45 Ma would have only resulted in only ca. 280 x
453 10^3 km^3 clastic volume exported to the Niger delta instead of the ca. 450 x 10^3 km^3 we estimated
454 (Table 1). This simple calculation supports that forcing by mantle dynamics is a first-order
455 process for enhancing the sediment export from the African continent (Burke et al, 2003).

456 West of the dashed line in Fig. 7, maximum denudation depths within the upwarp domain
457 suggest some rock uplift associated with flexure along the passive margin (Beauvais & Chardon,
458 2013; Grimaud et al., 2014). In detail, denudation histories vary across the different segments
459 along the margin, indicating a complex evolution. For example, erosion rates decreased along
460 major valleys of the Long Atlantic drainages between the 24-11 and 11-0 Ma intervals during the
461 progressive dissection of the upwarp, while they remained high in the Guinean Rise (i.e.
462 Senegambia and Short Atlantic drainages; Fig. 6). These different erosion dynamics resulted in
463 contrasted post-24 Ma evolution of clastic export rates in these drainage groups (Fig. 7b, 7c and
464 7d), resulting in source-to-sink systems that are not monotonous along the marginal upwarp. The
465 variability of erosion rates may tentatively be related to uplift rate variations along the continental
466 margin. Potentially, the stretching of a heterogeneous lithosphere or a non-cylindrical margin
467 during the rifting stage generates potentially complex, laterally variable uplift patterns, which
468 may be maintained long after rifting (Chardon et al., 2013; Rouby et al., 2013), leading to
469 unevenly distributed erosion rates.

470 Our analysis shows that dated relict lateritic landforms are reliable markers of post-rift
471 denudation of continental passive margins and adjacent cratonic domains with sufficient spatial
472 and temporal resolution. The variability of erosion histories along the margin shows (similarly to
473 Pazzaglia & Gardner (1994) along the US Atlantic margin) that modern topography and paleo-

474 denudation rates do not necessarily correlate (Figs. 2 and 7) and that independent geomorphic
475 markers are more robust than present-day digital elevation models to constrain surface dynamics
476 over geological timescales. West Africa is a non-orogenic domain where the erosion dynamics
477 may be compared to the adjoining offshore record thanks to a spatially constrained onshore
478 denudation chronology. In the future, new insights on the Cenozoic surface evolution of shields
479 and their bounding margins (e.g. Australia, Brazil, India, South Africa) will arise from the
480 mapping of relict landforms, whose lateritic cover has been dated using supergene minerals (e.g.
481 Vasconcelos et al., 1994a; 1994b; Vasconcelos & Conroy, 2003; Bonnet et al., 2014; 2016; Riffel
482 et al., 2015; Beauvais et al., 2016).

483

484 **CONCLUSIONS**

485 We have quantified patterns and volumes of Cenozoic denudation and catchment export using
486 dated and regionally correlated relict lateritic landforms of Sub-Saharan West Africa. Overall
487 denudation rates are regionally low in this non-orogenic domain (~7 m Myr^{-1}) but may increase
488 significantly locally with rock uplift, whether driven by mantle dynamics or lithosphere
489 deformation and flexure, as for example in the Hoggar hotspot swell and along a marginal
490 upwarp. Comparisons with clastic volumes accumulated offshore show a fairly balanced
491 sediment budget between the Niger catchment and its delta since 45 Ma. The Niger catchment
492 was established since at least 29 Ma and allowed transporting sufficient clastic material to the
493 delta; in particular by collecting the erosion products of the growing Hoggar hotspot swell.
494 Accumulations along the remaining Equatorial Atlantic margin of Africa suggest an apparent
495 export deficit from its source but our estimation is poorly constrained by available offshore data,
496 and complicated by potential sediment input from the Niger delta. Sediment reworking shredding

497 the depositional record is also suggested in several locations, prompting caution when deducing
498 continental denudation rates from accumulation only.

499

500 **Acknowledgement:**

501 This work was funded by WAXI, the CNRS and the ANR TopoAfrica (ANR-08-BLAN-572
502 0247–02) and supported by the gOcad consortium. We thank Michel Séranne and the SAFL
503 sediment dynamics group for fruitful discussions and suggestions as well as Damien Huygues
504 and Stéphane Perrouty for support. The manuscript also benefited from constructive reviews by
505 Frank Pazzaglia, Luc Lavier and Peter van der Beek. We acknowledge AMIRA International and
506 the industry sponsors, including AusAid and the ARC Linkage Project LP110100667, for their
507 support of the WAXI project (P934A) as well as the Geological Surveys/Departments of Mines
508 in West Africa as sponsors in kind of WAXI.

509

REFERENCES

ADEGOKE, O.S., AGUMANU, A.E., BENKHELIL, M.J. & AJAYI, P.O. (1986) New stratigraphic, sedimentologic and structural data on the kerri-kerri formation, Bauchi and Borno States, Nigeria. *J. Afr. Earth Sci.*, **5,** 249-277.

ALLEN, P.A. (2008) From landscapes into geological history. *Nature*, **451,** 274-276.

ANKA, Z., SÉRANNE, M., LOPEZ, M., SCHECK-WENDEROTH, M. & SAVOYE, B. (2009) The long-term evolution of the Congo deep-sea fan: A basin-wide view of the interaction between a giant submarine fan and a mature passive margin (ZaiAngo project). *Tectonophysics*, **470,** 42-56.

BEAUMONT, C., KOOI, H. & WILLETT, S. (2000) Coupled tectonic-surface process models with applications to rifted margins and collisional orogens. *In: Geomorphology and global tectonics* (Ed. by M. A. Summerfield), 29-55. John Wiley & Sons, Chichester UK

BEAUVAIS, A., BONNET, N.J., CHARDON, D., ARNAUD, N. & JAYANANDA, M. (2016) Very long-term stability of passive margin escarpment constrained by $^{40}Ar/^{39}Ar$ dating of K-Mn oxides. *Geology*, **44**, 299-302.

BEAUVAIS, A. & COLIN, F. (1993) Formation and transformation processes of iron duricrust systems in tropical humid environment. *Chem. Geol.*, **106,** 77-101.

BEAUVAIS, A., RUFFET, G., HÉNOCQUE, O. & COLIN, F. (2008) Chemical and physical erosion rhythms of the West African Cenozoic morphogenesis: The 39Ar-40Ar dating of supergene K-Mn oxides. *J. Geophys. Res.*, **113,** F04007**.**

BEAUVAIS, A. & CHARDON, D. (2013) Modes, tempo and spatial variability of Cenozoic cratonic denudation: The West African example. *Geochem. Geophys. Geosyst.*, **14,** 1590–1608.

BENKHELIL, J. (1989) The origin and evolution of the Cretaceous Benue Trough (Nigeria). *J. Afr. Earth Sci.*, **8,** 251-282.

BISHOP, P. (1995) Drainage rearrangement by river capture, beheading and diversion. *Prog. Phys. Geogr.*, **19**, 449-473.

BISHOP, P. (2007) Long-term landscape evolution: linking tectonics and surface processes. *Earth Surf. Proc. Land.*, **32,** 329-365.

BONNET N.J., BEAUVAIS, A., ARNAUD, N., CHARDON, D. & JAYANANDA, M. (2014) First $^{40}Ar/^{39}Ar$ dating of intense late Palaeogene lateritic weathering in Peninsular India. *Earth Planet. Sci. Letters*, **386**, 126-137.

BONNET N.J., BEAUVAIS, A., ARNAUD, N., CHARDON, D. & JAYANANDA, M. (2016) Cenozoic lateritic weathering and erosion history of Peninsular India from $^{40}Ar/^{39}Ar$ dating of supergene K-Mn oxides. *Chem. Geol.*, **446**, 33-53.

BOULANGÉ, B. & ESCHENBRENNER, V. (1971) Note sur la présence de cuirasses témoins des niveaux bauxitiques et intermédiaires, plateau de Jos Nigéria. *Bull. Ass. Sénég. Quatern. Ouest Afr.*, **31,** 83-92.

BOULANGÉ, B., SIGOLO, J.B. & DELVIGNE, J. (1973) Descriptions morphoscopiques, géochimiques et minéralogiques des faciès cuirassés des principaux niveaux géomorphologiques de Côte d'Ivoire. *Cah. ORSTOM, sér. Géol.*, **5,** 59-81.

BOULANGÉ, B. (1984) *Les formations bauxitiques latéritiques de Côte d'Ivoire; les faciès, leur transformation, leur distribution et l'évolution du modelé*. ORSTOM, Bondy, France.

BOULANGÉ, B. & MILLOT, G. (1988) La distribution des bauxites sur le craton ouest-africain. *Sci. Géol. Bull.*, **41,** 113-123.

555 BOWDEN, D.J. (1987) On the composition and fabric of the footslop laterites (duricrusts) of the
556 Sierra Leone, West Africa, and their geomorphological significance. *Z. Geomorphol.*
557 *Suppl.*, **64,** 39–53.
558 BRADLEY, D.C. (2008) Passive margins through earth history. *Earth-Sci. Rev.*, **91**, 1-26.
559 BROWNFIELD, M.E. & CHARPENTIER, R.R. (2006) Geology and total petroleum systems of
560 the Gulf of Guinea Province of West Africa. *U.S. Geol. Surv. Bulletin*, **2207-C**.
561 BURBANK, D.W. (1992) Causes of recent Himalayan uplift deduced from deposited patterns in
562 the Ganges basin. *Nature*, **357,** 680-683.
563 BURKE, K. (1976) The chad basin: An active intra-continental basin. *Tectonophysics*, **36,** 197-
564 206.
565 BURKE, K. (1996) The African Plate. *S. Afr. J. Geol.*, **99,** 339-409.
566 BURKE, K., MACGREGOR, D.S. & CAMERON, N.R. (2003) Africa's petroleum systems; four
567 tectonic 'aces' in the past 600 million years. In: *Petroleum Geology of Africa: New*
568 *Themes and Developing Technologies.* (Ed. by T. J. Arthur, D. S. MacGregor & N. R.
569 Cameron), *Geol. Soc. London Spec. Publ.*, **207**, 21-60.
570 CAMPANILE, D., NAMBIAR, C.G., BISHOP, P., WIDDOWSON, M. & BROWN, R. (2008)
571 Sedimentation record in the Konkan–Kerala Basin: implications for the evolution of the
572 Western Ghats and the Western Indian passive margin. *Basin Res.*, **20**, 3-22.
573 CHARDON, D., ROUBY, D., ROBIN, C., CALVES, G., GRIMAUD, J.L., GUILLOCHEAU,
574 F., BEAUVAIS, A. & BRAUN, J. (2013) Source to sink study of non-cylindrical rifted
575 passive margins: the case of the Gulf of Guinea. *Geophys. Res. Abstr.*, EGU2013-5223-1.
576 CHARDON, D., GRIMAUD, J.-L., Rouby, D., BEAUVAIS, A. & CHRISTOPHOUL, F. (2016)
577 Stabilization of large drainage basins over geological time scales: Cenozoic West Africa,
578 hot spot swell growth, and the Niger River. *Geochem. Geophys. Geosyst.*, **17**, 1164-1181.

579 CLIFT, P.D. (2010) Enhanced global continental erosion and exhumation driven by Oligo-
580 Miocene climate change. *Geophys. Res. Lett.*, **37,** L09402.
581 DE CAPRONA, G.C. (1992) *The continental margin of western Côte d'Ivoire: Structural*
582 *framework inherited from intra-continental shearing.* PhD Thesis. University of
583 Gothenburg. Gothenburg, Sweden.
584 DOUST, H. & OMATSOLA, E. (1990) Niger Delta. In: *Divergent/passive Margin Basins* (Ed.
585 by J. D. Edwards & P. A. Santogrossi), *AAPG Memoir*, **48**, 239-248.
586 DUROTOYE, B. (1989) Quaternary sediments in Nigeria. In: *Geology of Nigeria, 2nd edition*
587 (Ed. by C. A. Kogbe), 431–444. Rock View International, Paris, France.
588 EMERY, K.O., UCHUPI, E., PHILLIPS, J., BOWIN, C.O., & MASCLE, J. (1975) Continental
589 margin of Western Africa: Angola to Sierra Leone. *Am. Assoc. Pet. Geol. Bull.*, ***59***, 2209-
590 2265.
591 ESCHENBRENNER, R. & GRANDIN, G. (1970) La séquence de cuirasses et ses
592 différenciations entre Agnibiléfrou et Diébougou (Haute-Volta). *Cah. ORSTOM, Sér.*
593 *Géol.*, **2,** 205-246.
594 FEYBESSE, J.-L., BILLA, M., GUERROT, C., DUGUEY, E., LESCUYER, J.-L., MILESI, J.-P.
595 & BOUCHOT, V. (2006) The paleoproterozoic Ghanaian province: Geodynamic model
596 and ore controls, including regional stress modeling. *Precambrian Res.*, **149,** 149-196.
597 FÖLSTER, H. (1969) Late Quaternary erosion phases in SW Nigeria. *Bull. Ass. Sénég. Quatern.*
598 *Ouest Afr.*, **21,** 29–35.
599 FRITSCH, P. (1978) Chronologie relative des formations cuirassées et analyse géographique des
600 facteurs de cuirassement au Cameroun. *Trav. Doc. CEGET,* **33,** 114-132.
601 GILCHRIST, A.R. & SUMMERFIELD, M.A. (1990) Differential denudation and flexural
602 isostasy in formation of rifted-margin upwarps. *Nature*, **346**, 739-742.

GRANDIN, G. & HAYWARD, D.F. (1975) Aplanissements cuirassés de la péninsule de Freetown (Sierra-Léone). *Cah. ORSTOM, sér. Géol.*, **7,** 11-16.

GRANDIN, G. (1976) *Aplanissements cuirassés et enrichissement des gisements de manganèse dans quelques régions d'Afrique de l'Ouest*. ORSTOM, Paris, France.

GREIGERT, J. (1966) *Description des formations crétacées et tertiaires du Bassin des Iullemmeden (Afrique occidentale)*. Editions BRGM, Paris, France.

GRIMAUD, J.-L. (2014) *Dynamique long-terme de l'érosion en contexte cratonique: l'Afrique de l'Ouest depuis l'Eocène*. PhD Thesis, Toulouse University, Toulouse, France.

GRIMAUD, J.-L., CHARDON, D. & BEAUVAIS, A. (2014) Very long-term incision dynamics of big rivers. *Earth Planet. Sci. Lett.*, **405,** 74-84.

GRIMAUD, J.-L., CHARDON, D., METELKA, V., BEAUVAIS, A. & BAMBA, O. (2015) Neogene cratonic erosion fluxes and landform evolution processes from regional regolith mapping (Burkina Faso, West Africa). *Geomorphology*, **241,** 315-330.

GUILLOCHEAU, F., ROUBY, D., ROBIN, C., HELM, C., ROLLAND, N., LE CARLIER DE VESLUD, C. & BRAUN, J. (2012) Quantification and causes of the terrigeneous sediment budget at the scale of a continental margin: a new method applied to the Namibia–South Africa margin. *Basin Res.*, **24,** 3-30.

GUILLOCHEAU, F., CHELALOU, R., LINOL, B., DAUTEUIL, O., ROBIN, C., MVONDO, F., CALLEC, Y. & COLIN, J. P. (2015) Cenozoic landscape evolution in and around the Congo Basin: constraints from sediments and planation surfaces. In: *Geology and Resource Potential of the Congo Basin* (Ed. by M. J. de Wit, F. Guillocheau & M. C. J. de Wit), *Regional Geology Reviews*, 271-313. Springer Berlin Heidelberg, Berlin Germany.

HAACK, R.C., SUNDARARAMAN, P., DIEDJOMAHOR, J.O., XIAO, H., GANT, N.J., MAY, E.D. & KELSCH, K. (2000) Niger Delta petroleum systems, Nigeria. In: *Petroleum systems of South Atlantic margins* (Ed. by M. R. Mello & B. J. Katz), *AAPG Memoir*, **48**, 213–231.

HELM, C. (2009) *Quantification des flux sédimentaires anciens à l'échelle d'un continent : le cas de l'Afrique au Méso-Cénozoïque*. PhD Thesis. Rennes University, Rennes, France.

JERMANNAUD, P., ROUBY, D., ROBIN, C., NALPAS, T., GUILLOCHEAU, F. & RAILLARD, S. (2010) Plio-Pleistocene sequence stratigraphic architecture of the eastern Niger Delta: A record of eustasy and aridification of Africa. *Mar. Pet. Geol.*, **27,** 810-821.

JEROLMACK, D.J. & PAOLA, C. (2010) Shredding of environmental signals by sediment transport. *Geophys. Res. Lett.*, **37,** L19401.

KING, L.C. (1962) *The Morphology of the Earth*. Oliver and Boyd, Edinburgh, UK.

LABAILS, C., OLIVET, J.-L., ASLANIAN, D. & ROEST, W.R. (2010) An alternative early opening scenario for the Central Atlantic Ocean. *Earth Planet. Sci. Lett.*, **297**, 355-368.

LAVIER, L.L., STECKLER, M.S. & BRIGAUD, F. (2001) Climatic and tectonic controls on the Cenozoic evolution of the West African margin. *Mar. Geol.*, **178,** 63-80.

LETURMY, P., LUCAZEAU, F., & BRIGAUD, F. (2003) Dynamic interactions between the gulf of Guinea passive margin and the Congo River drainage basin: 1. Morphology and mass balance. *J. Geophys. Res.: Solid Earth*, **108**, 2156-2202.

LINOL, B., DE WIT, M.J., GUILLOCHEAU, F., DE WIT, M.C.J., ANKA, Z. & COLIN, J.-P. (2014) Formation and Collapse of the Kalahari Duricrust ['African Surface'] Across the Congo Basin, with Implications for Changes in Rates of Cenozoic Off-Shore Sedimentation. In: *Geology and Resource Potential of the Congo Basin* (Ed. by M. J. de

Wit, F. Guillocheau & M. C. J. de Wit), *Regional Geology Reviews*, 193-210. Springer Berlin Heidelberg, Berlin Germany.

MACGREGOR, D.S., ROBINSON, J. & SPEAR, G. (2003) Play fairways of the Gulf of Guinea transform margin. In: *Petroleum Geology of Africa: New Themes and Developing Technologies.* (Ed. by T. J. Arthur, D. S. MacGregor & N. R. Cameron), *Geol. Soc. London Spec. Publ.*, **207**, 131-150.

MACGREGOR, D.S. (2013) Late Cretaceous–Cenozoic sediment and turbidite reservoir supply to South Atlantic margins. *Spec. Publ. - Geol. Soc. London*, **369**, 109-128.

MALLET, J.L. (1992) Discrete smooth interpolation in geometric modelling. *Computer-Aided Design*, **24,** 178-191.

MÉTIVIER, F. & GAUDEMER, Y. (1999) Stability of output fluxes of large rivers in South and East Asia during the last 2 million years: implications on floodplain processes. *Basin Res.*, **11,** 293-303.

MÉTIVIER, F., GAUDEMER, Y., TAPPONNIER, P., & KLEIN, M., (1999) Mass accumulation rates in Asia during the Cenozoic. *Geophys. J. Int.*, **137**, 280-318.

MICHEL, P. (1973) *Les bassins des fleuves Sénégal et Gambie : étude géomorphologique*. ORSTOM, Paris, France.

MICHEL, P. (1977a) Les modelés et dépôts du Sahara méridional et Sahel et du Sud-Ouest africain. *Rech. Géograph. Strasbourg*, **5,** 5-39.

MICHEL, P. (1977b) Recherches sur le Quaternaire en Afrique occidentale. *Supp. Bull. AFEQ*, **50,** 143-153.

MILLOT, G. (1970) *Geology of Clays.* Springer Verlag, Berlin, Germany.

MOLNAR, P. (2004) Late Cenozoic increase in accumulation rates of terrestrial sediment: How Might Climate Change Have Affected Erosion Rates? *Annu. Rev. Earth Planet. Sci.*, **32,** 67-89.

MOULIN, M., ASLANIAN, D. & UNTERNEHR, P. (2010) A new starting point for the South and Equatorial Atlantic Ocean. *Earth-Sci. Rev.*, **98,** 1-37.

NEWILL, D. & DOWLING, J.W.F. (1968) Laterites in West Malaysia and Northern Nigeria. *Int. Conf. SMFE, Spec. Sess. on Eng. Propeties of Lateritic Soils*, **2,** 133-150.

PAZZAGLIA, F.J. & GARDNER, T.W. (1994) Late Cenozoic flexural deformation of the middle U.S. Atlantic passive margin. *J. Geophys. Res.: Solid Earth*, **99,** 12143-12157.

RADIER, H. (1959) *Contribution à l'étude géologique du Soudan oriental (AOF). 2 Le bassin crétacé et tertiaire de Gao le détroit soudanais*. Service de géologie et de prospection minière, Dakar, Sénégal.

REIJERS, T. (2011) Stratigraphy and sedimentology of the Niger Delta. *Geologos*, **17,** 133-162.

RIFFEL, S. B., VASCONCELOS, P. M., CARMO, I. O. & FARLEY, K. A. (2015) Combined 40Ar/39Ar and (U–Th)/He geochronological constraints on long-term landscape evolution of the Second Paraná Plateau and its ruiniform surface features, Paraná, Brazil, *Geomorphology*, **233**, 52-63.

ROBIN, C., GUILLOCHEAU, F., JEANNE, S., PORCHER, F. & CALVÈS, G. (2011) Cenozoic siliciclastic fluxes evolution around Africa. *Geophys. Res. Abstr.*, **13**, EGU2011-5659.

ROGNON, P., GOURINARD, Y., BANDET, Y., KOENIGUER, J.C. & DELTEIL-DESNEUX, F. (1983) Précisions chronologiques sur l'évolution volcanotectonique et

géomorphologique de l'Atakor (Hoggar); apports des données radiométriques (K/Ar) et paléobotaniques (bois fossiles). *Bull. Soc. Géol. Fr.*, **25,** 973-980.

ROUBY, D., BONNET, S., GUILLOCHEAU, F., GALLAGHER, K., ROBIN, C., BIANCOTTO, F., DAUTEUIL, O. & BRAUN, J. (2009) Sediment supply to the Orange sedimentary system over the last 150 My: An evaluation from sedimentation/denudation balance. *Mar. Pet. Geol.*, **26,** 782-794.

ROUBY, D., BRAUN, J., ROBIN, C., DAUTEUIL, O. & DESCHAMPS, F. (2013) Long-term stratigraphic evolution of Atlantic-type passive margins: A numerical approach of interactions between surface processes, flexural isostasy and 3D thermal subsidence. *Tectonophysics*, **604,** 83-103.

ROUGIER, S., MISSENARD, Y., GAUTHERON, C., BARBARAND, J., ZEYEN, H., PINNA, R., LIÉGEOIS, J.-P., BONIN, B., OUABADI, A., DERDER, M.E.-M. & DE LAMOTTE, D.F. (2013) Eocene exhumation of the Tuareg Shield (Sahara Desert, Africa). *Geology*, **41,** 615-618.

SADLER, P.M. (1981) Sediment accumulation rates and the completeness of stratigraphic sections. *J. Geol.*, **89,** 569–584.

SÉRANNE, M. (1999) Early Oligocene stratigraphic turnover on the west Africa continental margin: a signature of the Tertiary greenhouse-to-icehouse transition? *Terra Nova*, **11,** 135-140.

SÉRANNE, M. & NZÉ ABEIGNE, C.-R. (1999) Oligocene to Holocene sediment drifts and bottom currents on the slope of Gabon continental margin (west Africa): Consequences for sedimentation and southeast Atlantic upwelling. *Sed. Geol.*, **128,** 179-199.

SIMOES, M., BRAUN, J. & BONNET, S. (2010) Continental-scale erosion and transport laws: A new approach to quantitatively investigate macroscale landscapes and associated

716 sediment fluxes over the geological past. *Geochem. Geophys. Geosyst.*, **11**, Q09001,
717 doi:10.1029/2010GC003121
718 TARDY, Y. & ROQUIN, C. (1998) *Dérive des continents, paléoclimats et altérations tropicales*.
719 BRGM, Orléans, France.
720 TEEUW, R.M. (2002) Regolith and diamond deposits around Tortiya, Ivory Coast, West Africa.
721 *CATENA*, **49,** 111-127.
722 THOMAS, M.F. (1980) *Timescales of landform development on tropical shields; a study from*
723 *Sierra Leone*. In: *Timescales in Geomorphology* (Ed. by R.A Cullingford, D.A. Davidson
724 & J. Lewin), 333-354. John Wiley & Sons, Chichester, UK.
725 THOMAS, M.F. (1994) *Geomorphology in the Tropics: A Study of Weathering and Denudation*
726 *in Low Latitudes*. John Wiley & Sons, New York, US.
727 VALETON, I. (1991) Bauxites and associated terrestrial sediments in Nigeria and their position
728 in the Bauxite belts of Africa. *J. Afr. Earth Sci.*, **12,** 297-310.
729 VASCONCELOS, P.M. & CONROY, M. (2003) Geochronology of weathering and landscape
730 evolution, Dugald River valley, NW Queensland, Australia. *Geochim. Cosmochim. Acta*,
731 **67**, 2913–2930. doi:10.1016/S0016-7037(02)0137
732 VASCONCELOS, P.M., BRIMHALL, G.H., BECKER, T.A. & RENNE, P.R. (1994a) $^{40}Ar/^{39}Ar$
733 analysis of supergene jarosite and alunite: Implications to the paleoweathering history of
734 the western USA and West Africa. *Geochim. Cosmochim. Acta*, **58,** 401-420.
735 VASCONCELOS, P.M., RENNE, P.R., BRIMHALL, G.H. & BECKER, T.A. (1994b) Direct
736 dating of weathering phenomena by $^{40}Ar/^{39}Ar$ and K-Ar analysis of supergene K-Mn
737 oxides. *Geochim. Cosmochim. Acta*, **58**, 1635–1665. doi:10.1016/0016-7037(94)9056

738 VILLENEUVE, M. (2005), Paleozoic basins in West Africa and the Mauritanide thrust belt. *J.*
739 *Afr. Earth Sci.*, 43(1-3), 166-195.
740 WALFORD, H.L. & WHITE, N.J. (2005) Constraining uplift and denudation of west African
741 continental margin by inversion of stacking velocity data. *J. Geophys. Res.*, **110,** B04403.
742 WINDOM, H.L. (1975) Eolian contributions to marine sediments. *J. Sediment. Res.*, **45,** 520-529.
743 YE, J., CHARDON, D., ROUBY, D., GUILLOCHEAU, F., DALL'ASTA, M., FERRY, J.N. &
744 BROUCKE, O. (2017) Paleogeographic and structural evolution of northwestern Africa
745 and its Atlantic margins since the Early Mesozoic. *Geosphere*, **13**, in press.
746 doi:10.1130/GES01426.1
747 ZACHOS, J., PAGANI, M., SLOAN, L., THOMAS, E. & BILLUPS, K. (2001) Trends,
748 Rhythms, and Aberrations in Global Climate 65 Ma to Present. *Science,* **292,** 686-693.
749

750 **FIGURES CAPTIONS**

751 Fig. 1: Schematic representation of a source-to-sink system with the riverine transport of
752 sediment from the continent to the ocean. The figure focuses on the clastic flux and does not
753 represent the solute load.

754

755 Fig. 2: Map showing the main geologic and morphologic features of Sub-Saharan West Africa
756 modified after Grimaud et al. (2014). The offshore accumulation map of Emery et al. (1975) does
757 not cover the Central Atlantic margin of Africa (i.e. offshore Senegal-Mauritania basin).

758

Fig. 3: Denudation chronology of Sub-Saharan West Africa during the Cenozoic. [a] Distribution of lateritic paleo-landsurfaces and associated regoliths (weathering mantles and associated duricrusts) in the landscape. [b] Comparison of the ages acquired in the lateritic mantles of Tambao and Syama, (Fig. 2) [after Beauvais et al. (2008) (light grey dots) and Vasconcelos et al. (1994a) (dark grey dots) respectively] to the oceanic $\delta^{18}O$ variation (‰) on benthic foraminifera tests recording global temperature variations (Zachos et al., 2001). Only the ages with an uncertainty lower than 5 Myr have been reported in Syama (dark grey dots).

Fig. 4: Interpretation of paleo-landsurface distribution after our field work in several type-locations in West Africa (see location on Fig. 2). Google-Earth view and interpretation of paleo-surface distribution: [a] over the Precambrian basement, South of Tambao (Burkina Faso); [b] over the Precambrian basement near the Manding Mounts (Mahadougou, Mali); [c] in the Niger inland delta, North of Bamako (Ségou, Mali) where bauxitic remnants are found 60 m above the Niger River; [d] in the Iullemmeden basin (North of Niamey, Niger) where the deposits of the "Continental Terminal", capped with the Intermediate surface, have been incised by the Niger River system. The color code of relict landforms interpretations is similar to Fig. 3.

Fig. 5: [a] Map of the ~2900 data points used to build the 3D surfaces. [b] Schematic distribution of relict landforms and reconstructed surface geometries. [c] Schematic distribution of data points constraining the construction of surface geometries in alluvial plains and sedimentary basins. B points correspond to bedrock massifs summit (referred as "inselbergs"), C points to the top of Early-Mid Eocene carbonates and D points to S1 weathering profile remnants. B points inselbergs are often associated with eroded S1 weathering profiles. B points therefore constrain

S1 minimum elevation. C points are time equivalents of S1 bauxite retrieved from well log in sedimentary basins. We used them as depth of S1 below the topography in these basins. D points constrain locally the elevation of S1 paleo-surface, which have been eroded, on the basis that a bauxitic weathering profile cannot exceed the maximum depth of 120 m (estimates based on electric profiles; Boulangé et al., 1973).

Fig. 6: [a] Simplified map of the 4 selected drainage groups (bounded by black lines): Senegambia drainage, Short Atlantic drainages, Long Atlantic drainages and the Niger catchment. The modern limits of the Cenozoic onshore sedimentary basins (Senegal-Mauritania [S.M.], Iullemmeden [Iu.] and Togo-Benin [T.B] basins) (red dashed lines) and main topographic massifs (Tagant [Tag.], Hoggar [Hog.], Guinean Rise [G.R.] Jos plateau [Jos] and Adamaoua massif [Ad.]) (grey areas) are also shown. Denudations maps of the 45-24 Ma [b], 24-11 Ma [c] and 11-0 Ma intervals [d]. Successive divides (black dashed lines) are drawn after Chardon et al. (2016). Where the position of these divides was less constrained, the uncertainty area is represented between two dashed lines.

Fig. 7: Cenozoic denudation map and associated exported volumes. [a] Map of total denudation depth at the scale of Sub-Saharan West Africa since the abandonment of S1. Clastic export rates are shown by drainage groups (i.e. Senegambia drainage [b], Short Atlantic drainages [c], Long Atlantic drainages [d] and the Niger catchment [e]). The eastern swells are separated from the rest of the study area by the black dashed line.

Fig. 8: Regional cross-sections of lateritic relict landforms distribution and contemporary sedimentary deposits (see Fig. 5 for location). [a] Cross-section through the Hoggar massif and Iullemmeden basin. [b] Cross section through the Benue trough and onshore Niger delta (geology after Benkhelil, 1989; volcanic accumulation in the Hoggar massif after Rognon et al., 1983). The red, purple and green dashed lines represent large-scale interpolations of the S1, S2 and S3 surfaces, respectively.

Fig. 9: Offshore accumulation histories. [a] 3D topography and bathymetry showing the location of the cross sections used in the study. [b] Example of cross-section for the Niger delta (after Haack et al., 2000). [c] Example of cross-section for the sediment accumulation offshore Ivory Coast (after Helm, 2009; see Supporting Information). [d] Evolution of volumetric accumulation rates in the Niger delta (after Haack et al., 2000 and Robin et al., 2011). [e] Evolution of volumetric accumulation rates in the Niger delta after time re-sampling in order to compare to the continental denudation chronology (i.e. 45-23, 23-11.6 and 11.6-0 Ma; see Table 2). [f] Evolution of volumetric accumulation rates on the African margin of the Equatorial Atlantic (modified after Helm 2009). See methods section and Supporting Information for details. Error bars include a Monte Carlo estimation of uncertainties related to sections interpolation, as well as non-clastic material (i.e. carbonates and volcanics) and porosity corrections.

Location	Interval	Eroded volume	Average equivalent denudation		Exported volume		Clastic export rate	Clastic yield
			depth	rate	total (V_{ex})	clastic (V_c)		
		(10^3 km^3)	(m)	(m Myr^{-1})	(10^3 km^3)		(10^3 m^3 Myr^{-1})	(t km^{-2} yr^{-1})
West Africa	*45-0 Ma*	1149	333	7,4	1112	834	18,5	13
Senegambia	*45-24 Ma*	39 5	74 3	3,5 0,1	30 5	22 4	1,1 0,2	4 1
	24-11 Ma	29 12	40 14	3,1 1,1	29 12	22 9	1,7 0,7	6 3
	11-0 Ma	40 5	59 8	5,3 0,7	40 5	30 4	2,7 0,4	11 1
Short Atlantic drainages	*45-24 Ma*	45 4	154 8	7,3 0,4	45 4	34 3	1,6 0,1	14 1
	24-11 Ma	37 7	119 19	9,2 1,4	37 7	27 5	2,1 0,4	19 4
	11-0 Ma	29 4	104 14	9,5 1,3	29 4	22 3	2,0 0,3	19 3
Long Atlantic drainages	*45-24 Ma*	99 41	197 17	9,4 0,8	97 40	73 30	3,5 1,4	17 4
	24-11 Ma	86 22	98 18	7,5 1,4	86 22	64 17	5,0 1,3	15 4
	11-0 Ma	44 7	53 8	4,8 0,8	44 7	33 5	3,0 0,5	9 1
Niger	*45-24 Ma*	196 178	138 31	6,6 1,5	153 136	115 102	5,5 4,8	7 5
	24-11 Ma	260 83	135 40	10,4 3,1	260 83	195 62	15,0 4,8	20 7
	11-0 Ma	177 11	86 5	7,8 0,5	177 11	133 8	12,1 0,7	15 1
Total Niger	*45-0 Ma*	633 271	359 76	8,2 1,7	591 229	443 172	10,9 3,4	14 4
Benue estimation	*45-0 Ma*			7,4		187		
Total Niger & Benue	*45-0 Ma*					**630 172**		

823

824 Table 1: Summary of Cenozoic erosion budgets of Sub-Saharan West Africa

825

	Interval	Accumulated volume
	(Ma)	(10^3 km^3)
S3 - modern	1.8 - 0	46.8 ± 6.3
	5.3 - 1.8	142.3 ± 19.9
	11.6 - 5.3	127.7 ± 17.8
S2 - S3	16 - 11.5	85.4 ± 11.9
	23 - 11.5	61 ± 8.5
S1 - S2	33.9 - 23	69.8 ± 10.4
	45 - 33.9	44.4 ± 15.7
	55.8 -33.9	87.6 ± 30.9
	Total 45-0	577.4 ± 90.5

826

827 Table 2: Summary of Cenozoic clastic volumes accumulated in the Niger delta.

828

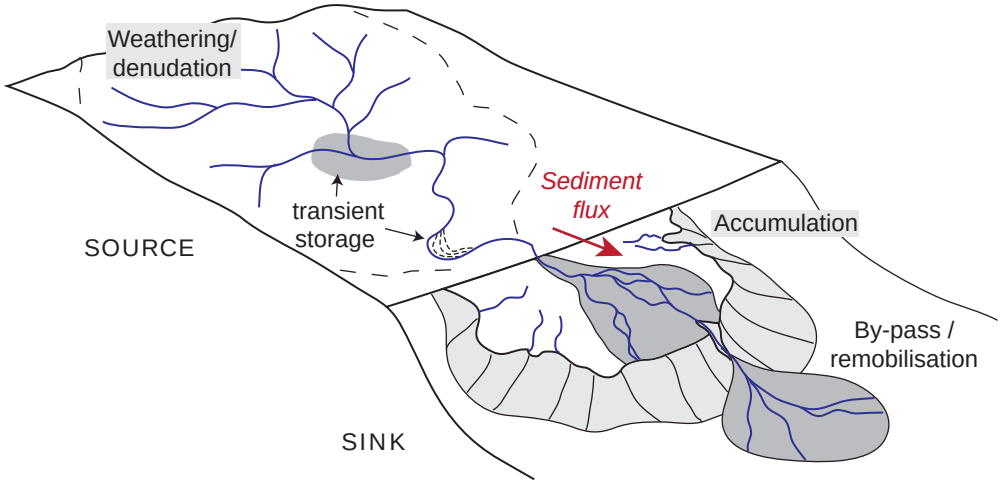

Grimaud et al., Fig. 1

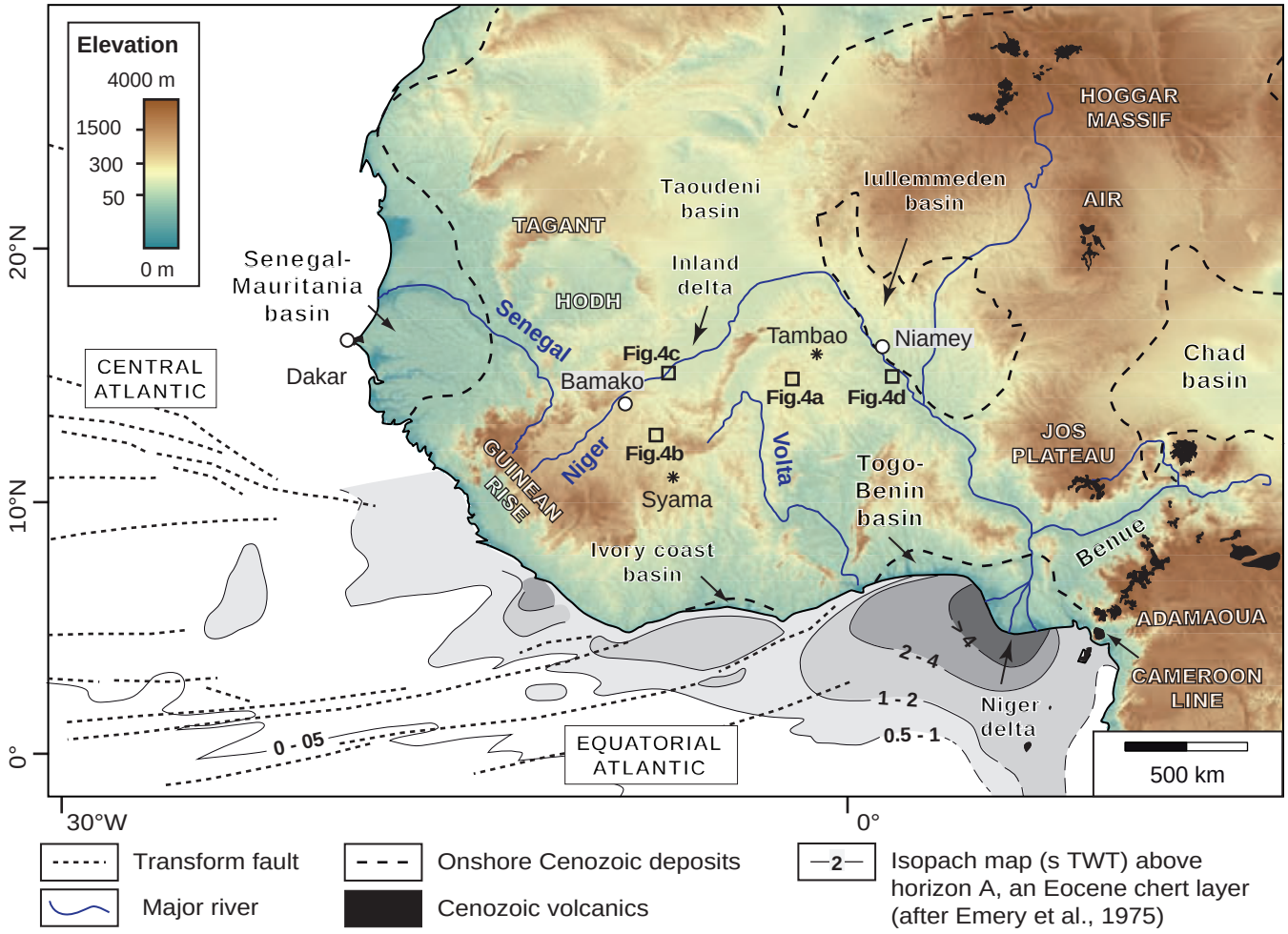

Grimaud et al., Fig. 2

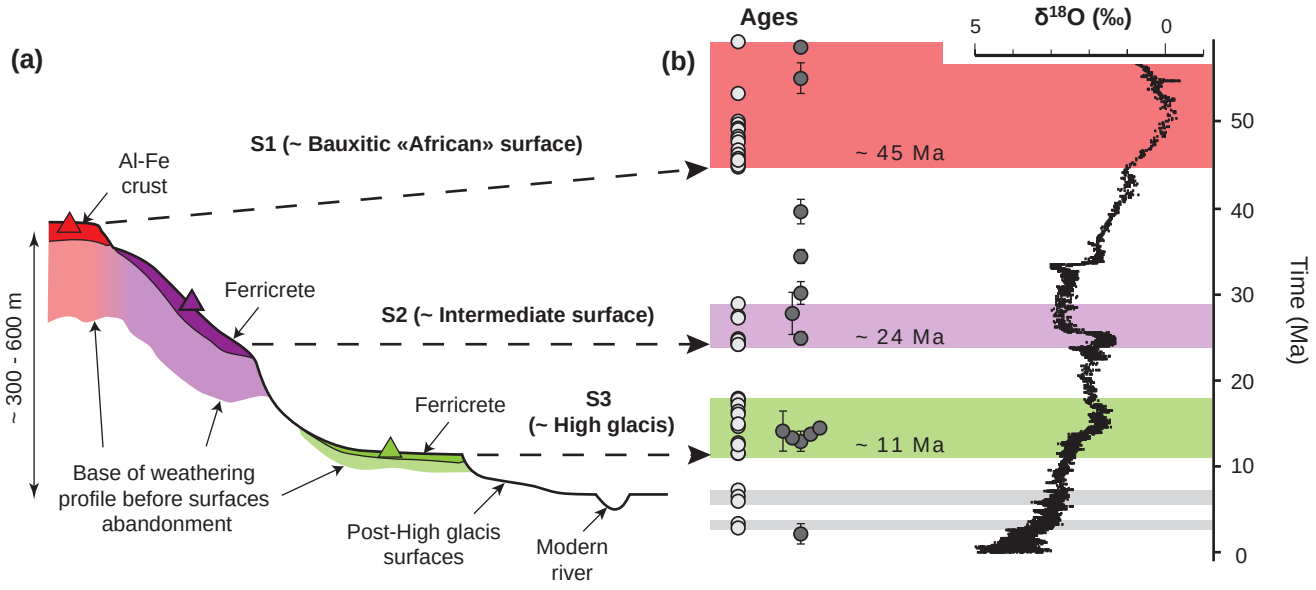

Grimaud et al., Fig. 3

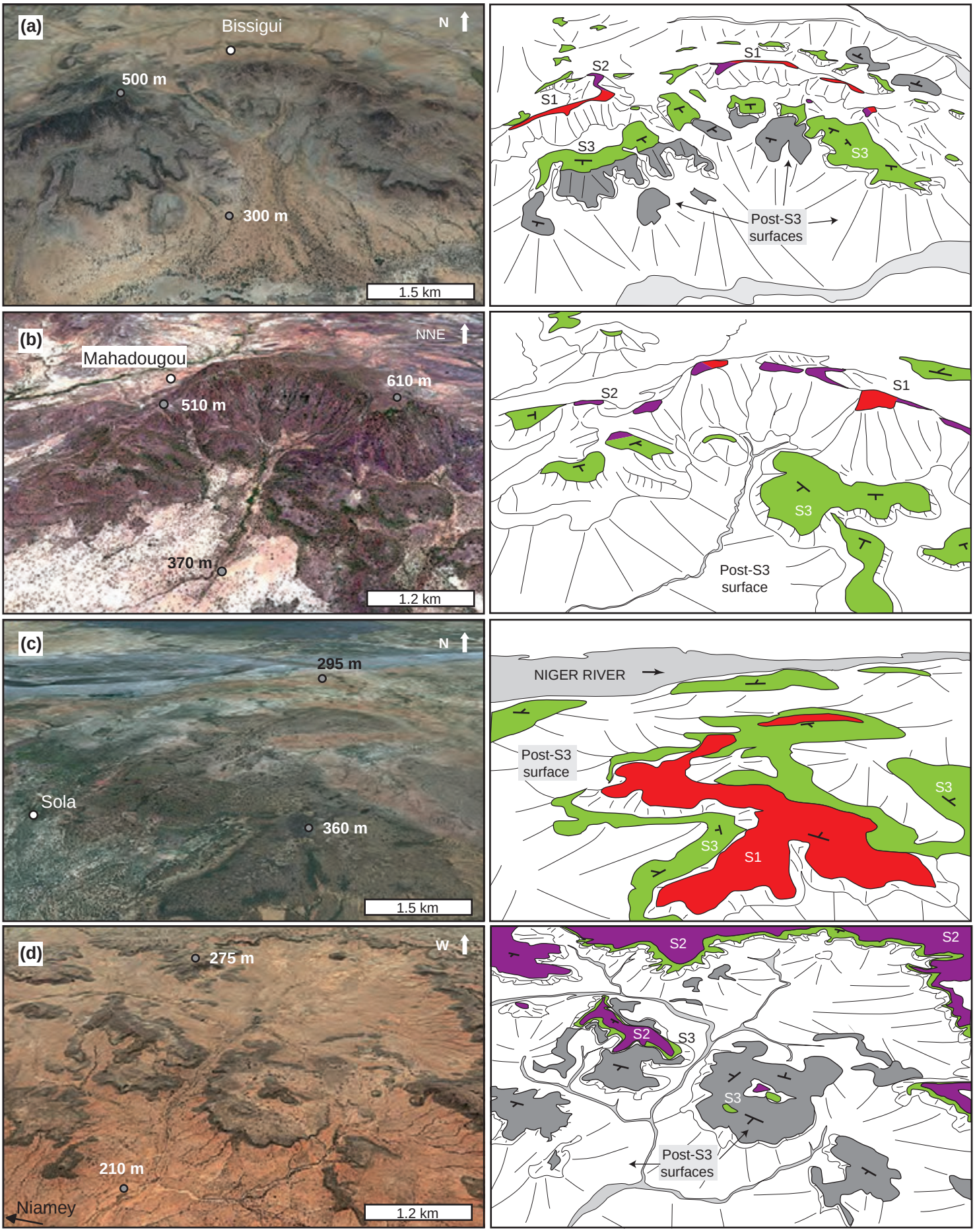

Grimaud et al., Fig. 4

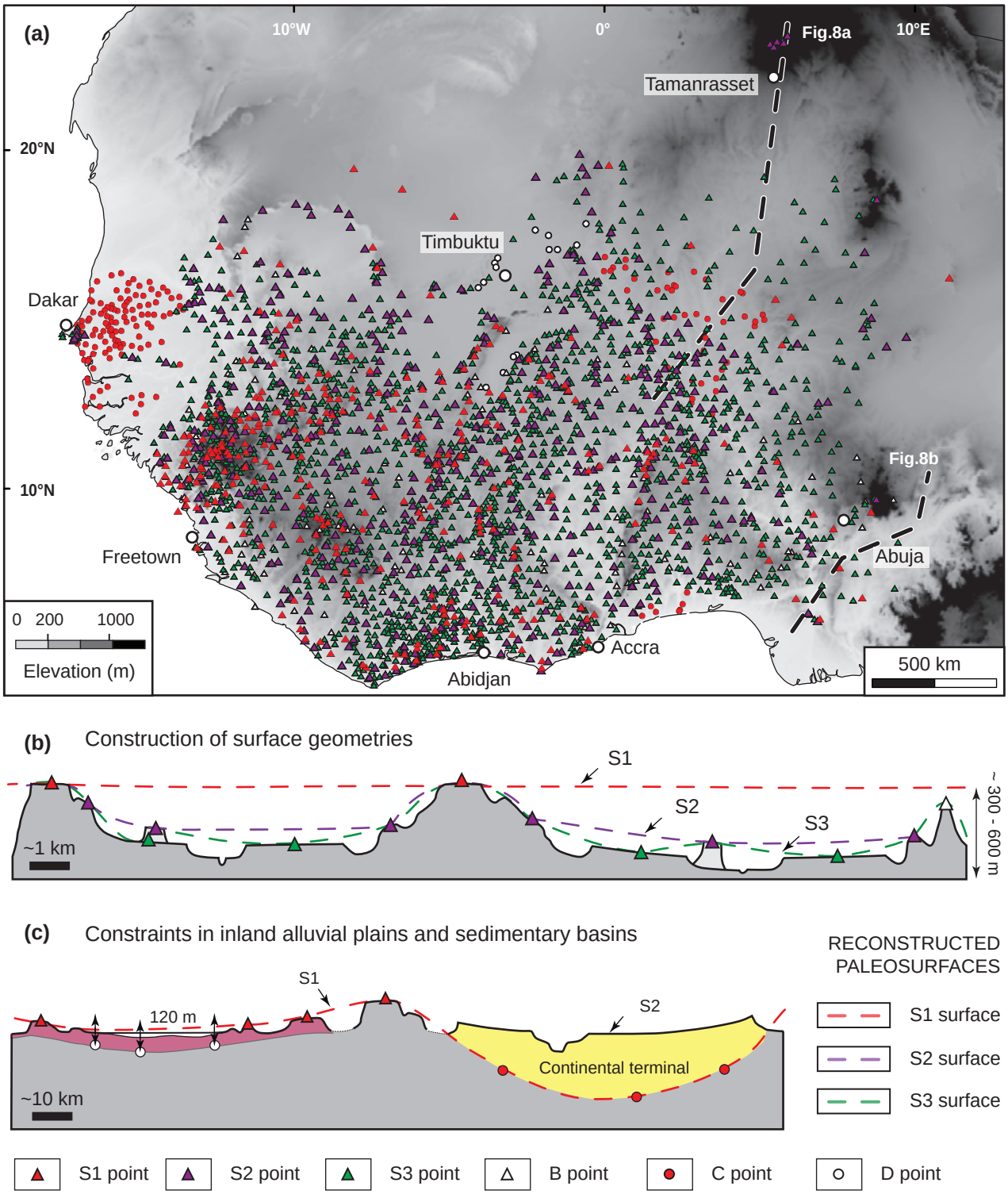

Grimaud et al., Fig. 5

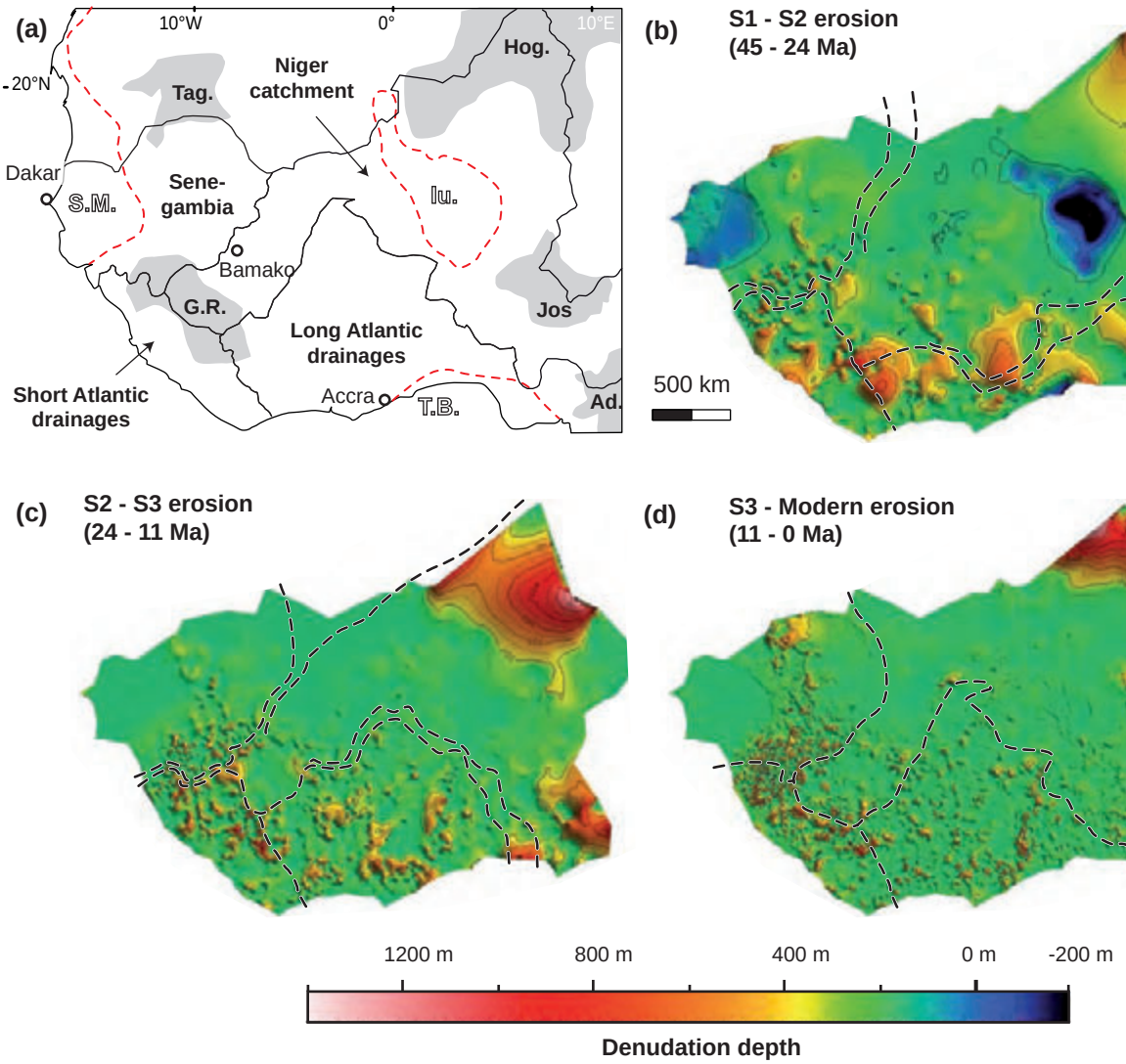

Grimaud et al., Fig. 6

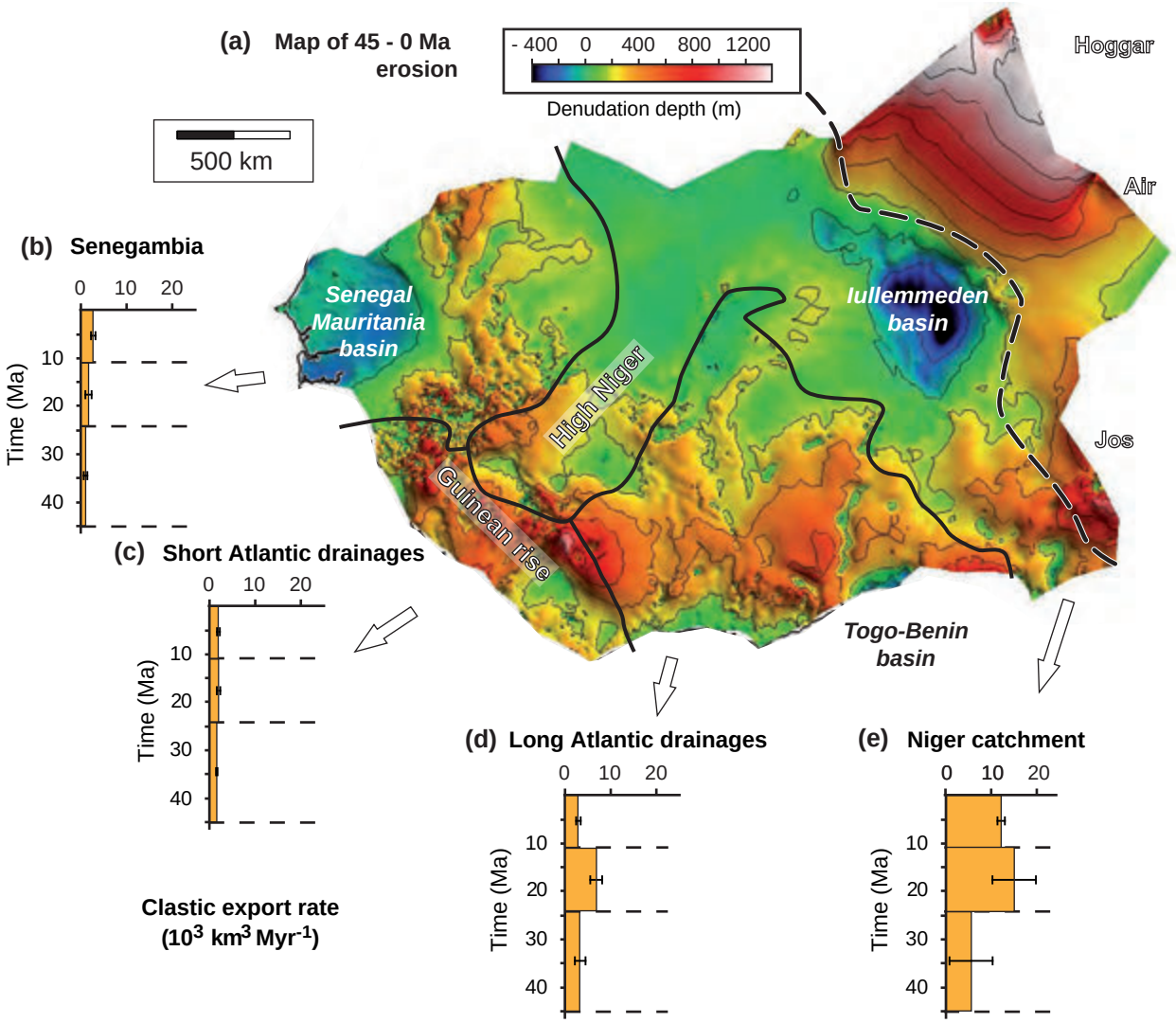

Grimaud et al., Fig. 7

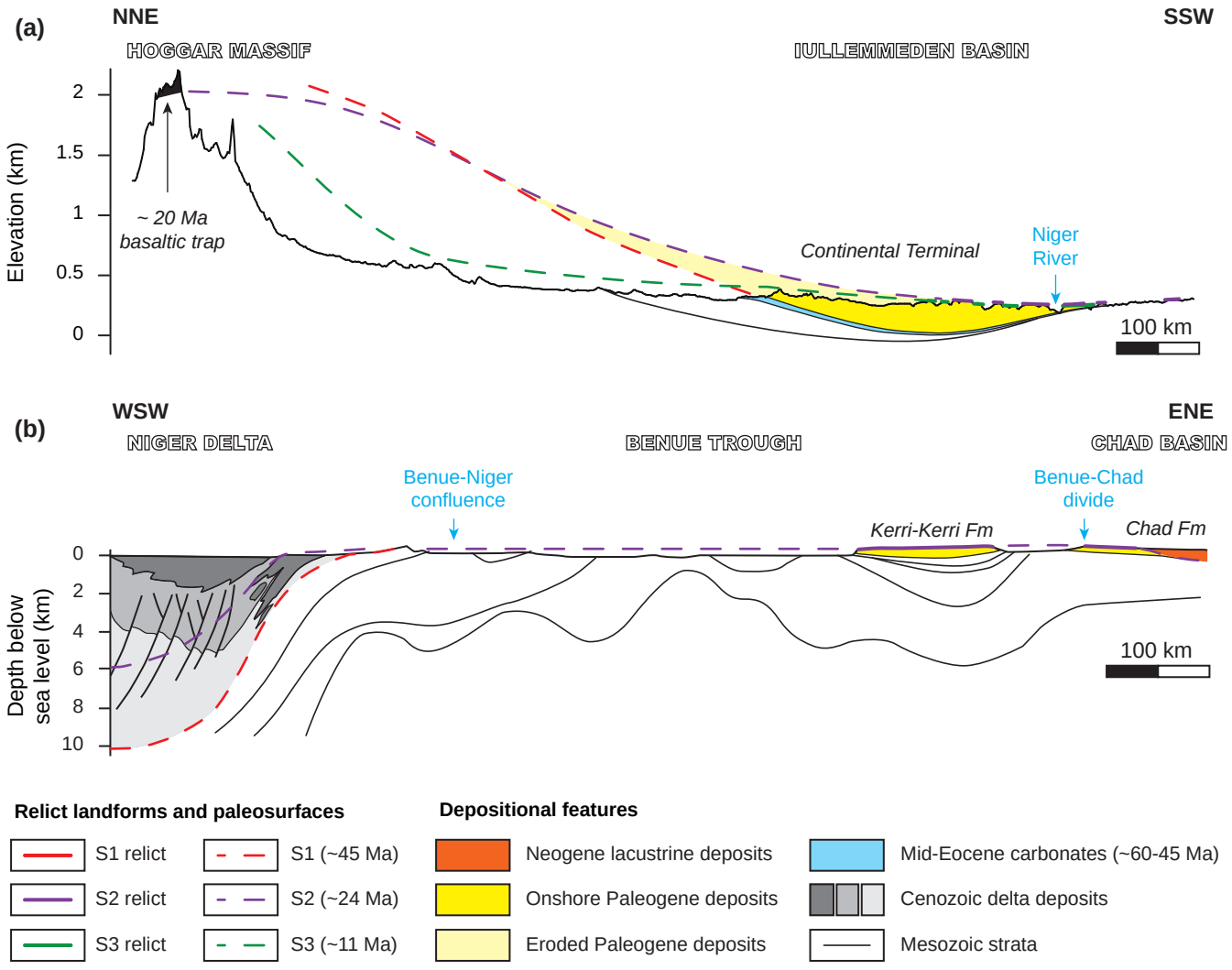

Grimaud et al., Fig. 8

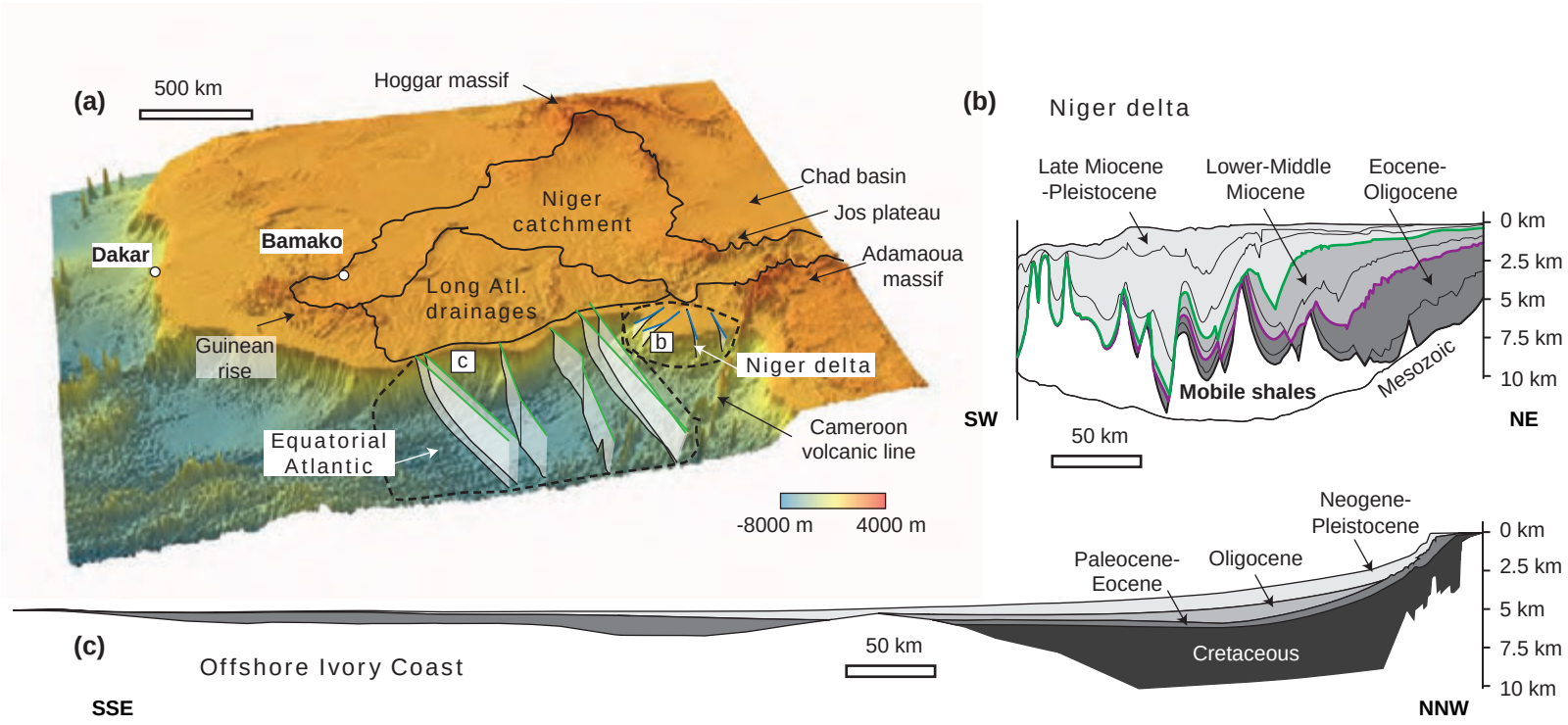

Accumulation rates (10^3 km^3 Myr^{-1})

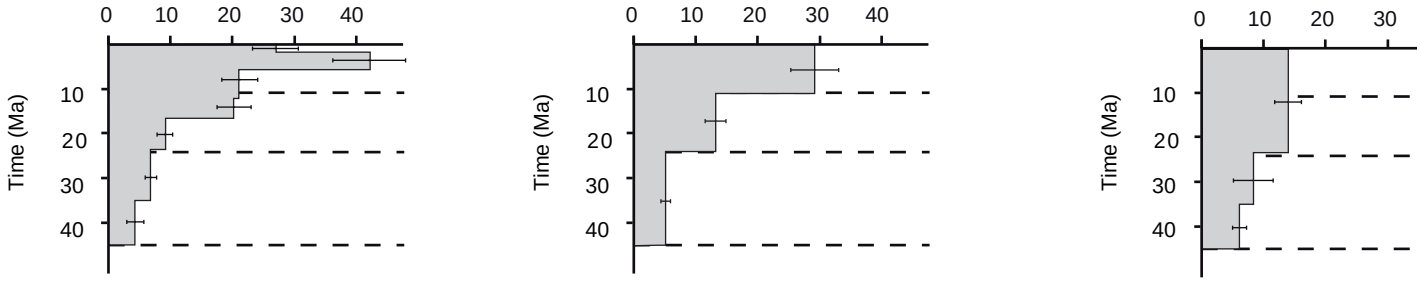

Grimaud et al., Fig. 9